How the Ligand Field in Lanthanide Coordination Complexes Determines Magnetic Susceptibility Anisotropy, Paramagnetic NMR Shift and Relaxation Behaviour

David Parker[1], Elizaveta A. Suturina[2], Ilya Kuprov[3], Nicholas F. Chilton[4]*

[1]Department of Chemistry, Durham University, South Road, Durham DH1 3LE, UK

[2]Department of Chemistry, University of Bath, Claverton Down, BA2 7AY, UK

[3]School of Chemistry, University of Southampton, Southampton, SO17 1BJ, UK

[4]Department of Chemistry, School of Natural Sciences, The University of Manchester, Manchester, M13 9PL, UK

email; david.parker@dur.ac.uk

TOC Graphic

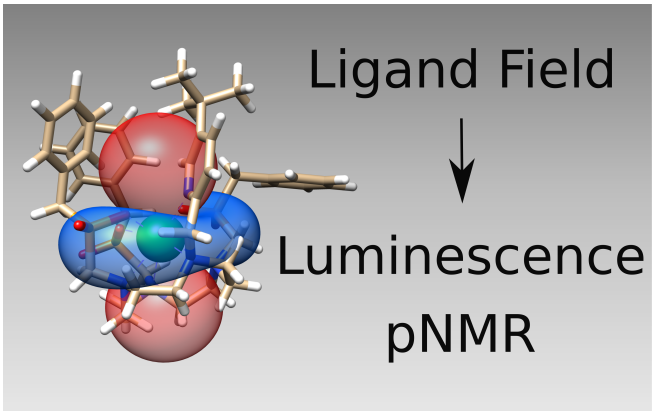

CONSPECTUS

Complexes of lanthanide(III) ions are being actively studied because of their unique ground and excited state properties, and the associated optical and magnetic behaviour. In particular, they are used as emissive probes in optical spectroscopy and microscopy, and as contrast agents in magnetic resonance imaging (MRI). However, the design of new complexes with specific optical and magnetic properties requires a thorough understanding of the correlation between molecular structure and electric and magnetic susceptibilities, as well as their anisotropies. The traditional Judd-Ofelt-Mason theory has failed to offer useful guidelines for systematic design of emissive lanthanide optical probes. Similarly, Bleaney's theory of magnetic anisotropy and its modifications fail to provide the accurate detail that permits new paramagnetic shift reagents to be designed rather than discovered.

A key determinant of optical and magnetic behaviour in *f*-element compounds is the ligand field, often considered as an electrostatic field at the lanthanide, created by the ligands. The resulting energy level splitting is a sensitive function of several factors: the nature and polarizability of the whole ligand and its donor atoms; the geometric details of the coordination polyhedron; the presence and extent of solvent interactions; specific hydrogen bonding effects on donor atoms and the degree of supramolecular order in the system. The relative importance of these factors can vary widely for different lanthanide ions and ligands. For nuclear magnetic properties, it is both the ligand field splitting and the magnetic susceptibility tensor, notably its anisotropy, that determine paramagnetic shifts and nuclear relaxation enhancement.

We review the factors that control the ligand field in lanthanide complexes and link these to aspects of their utility in magnetic resonance and optical emission

spectroscopy and imaging. We examine recent progress in this area particularly in the theory of paramagnetic chemical shift and relaxation enhancement, where some long-neglected effects of zero-field splitting, magnetic susceptibility anisotropy and spatial distribution of lanthanide tags have been accommodated in an elegant way.

KEY REFERENCES

(1) Suturina, E. A.; Mason, K.; Geraldes, C. F.; Kuprov, I.; Parker, D. Beyond Bleaney's Theory: Experimental and Theoretical Analysis of Periodic Trends in Lanthanide-Induced Chemical Shift. *Angewandte Chemie International Edition* **2017**, *56*, 12215-12218. The orientation of the main component of the magnetic susceptibility tensor differs significantly for lanthanide complexes of a common ligand; thus, one of the key assumptions in Bleaney's theory is incorrect.

(2) Vonci, M.; Mason, K.; Suturina, E. A.; Frawley, A. T.; Worswick, S. G.; Kuprov, I.; Parker, D.; McInnes, E. J.; Chilton, N. F. Rationalization of Anomalous Pseudocontact Shifts and Their Solvent Dependence in a Series of C_3-Symmetric Lanthanide Complexes. *Journal of the American Chemical Society* **2017**, *139*, 14166-14172. The sign and magnitude of the pseudocontact chemical shift, determined by the anisotropy of the magnetic susceptibility tensor, can be extremely sensitive to minimal structural changes, such as differential complex solvation.

(3) Harnden, A. C.; Suturina, E. A.; Batsanov, A. S.; Senanayake, P. K.; Fox, M. A.; Mason, K.; Vonci, M.; McInnes, E. J.; Chilton, N. F.; Parker, D. Unravelling the Complexities of Pseudocontact Shift Analysis in Lanthanide Coordination Complexes of Differing Symmetry. *Angewandte Chemie International Edition* **2019**, *131*, 10396-10400. A switch in the sign of the dominant ligand field paramater and large changes in the sense, amplitude and orientation of the main component of the magnetic susceptibility tensor may occur simultaneously and hence hide smaller NMR pseudocontact shift changes.

(4) Suturina, E. A.; Mason, K.; Geraldes, C. F.; Chilton, N. F.; Parker, D.; Kuprov, I. Lanthanide-induced relaxation anisotropy. *Physical Chemistry Chemical Physics* **2018**, *20*, 17676-17686. Detailed variable field proton relaxation rate analyses for isostructural series of lanthanide complexes reveal an angular dependence in both the dipolar and Curie mechanisms, demonstrated both experimentally and theoretically in a revised approach.

ELECTRONIC STRUCTURE INTRODUCTION

The unique electronic structure of trivalent 4*f* ions determines the distinctive properties of their coordination complexes. The electrostatic shielding of the electrons in 4*f* orbitals by fully occupied 5*s* and 5*p* orbitals makes the effects from surrounding ligands and other molecules far smaller than the inter-electron repulsion and spin-orbit coupling (

Figure 1). Due to these order-of-magnitude differences, electronic transitions in lanthanide(III) complexes are often independent of the ligand environment and the ligand field splitting can be considered on the basis of the ground-state total angular momentum, *J*.

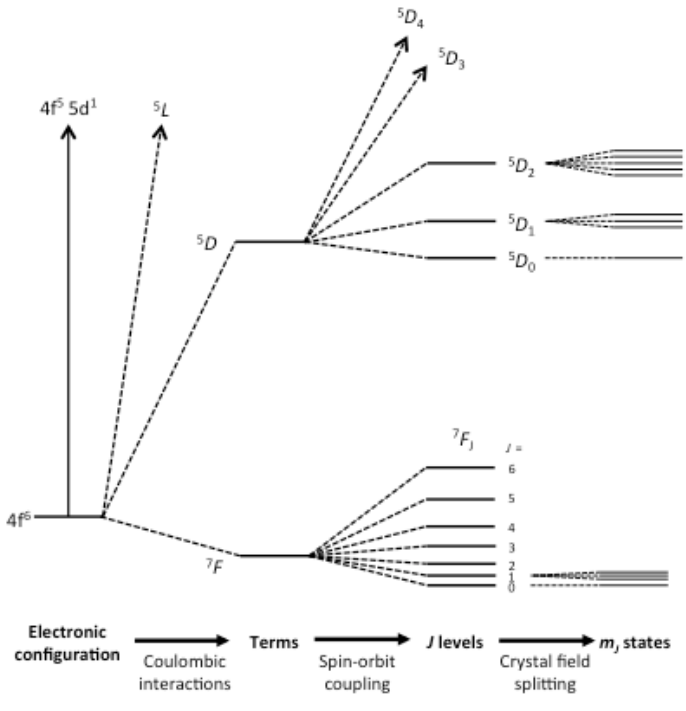

Figure 1. Schematic representation of electronic states for Eu(III) ($4f^6$): six electrons occupy seven degenerate 4f orbitals giving a ^7F ground term in the Russell-Saunders coupling scheme (spectroscopic notation, $^{2S+1}L_J$), with total spin $S = 3$ and total orbital angular momentum $L = 3$. Spin-orbit coupling splits this term into seven J multiplets separated by about 10^3 cm^{-1}. Each J state is $2J+1$-fold degenerate for the free-ion; this degeneracy is partially removed upon loss of spherical symmetry. The separation of m_J states due to the ligand field is around 10^2 cm^{-1}, but can be much larger.

The energy of m_J sublevels can be calculated using the crystal field theory that neglects mixing of *f*-orbitals with the orbitals of the ligands. For a given J multiplet, the model Hamiltonian has the form given in eq. 1:

$$\hat{H} = \sum_{k=2,4,6} \theta_k \sum_{q=-k}^{k} B_q^k \hat{O}_k^q \qquad (1)$$

where B_q^k are ligand field parameters, O_k^q are Stevens operators, and θ_k are operator equivalent coefficients (Table 1), defined for each term and multiplet in a given configuration.[5,6] The B_q^k parameters are defined in a particular reference frame; in symmetric molecules, the z-axis is usually aligned with the principal axes of the symmetry group, in which case the number of non-zero parameters is reduced.[7,8] In the absence of symmetry, the expansion in Eq (1) has 27 independent parameters. However, given sufficiently high symmetry and/or enough spectroscopic data, all non-zero ligand field parameters may be determined by luminescence spectroscopy.[9,10] The principal parameter of interest to the NMR community is B_0^2, due to the prevalence of Bleaney's theory.[11] As an example, for Eu(III), it may be

extracted directly from the $^5D_0$ to $^7F_1$ transition (Figure 2).[12-14] The B_q^k parameters can be estimated from experimental data, but are nowadays commonly obtained from multi-reference *ab initio* electronic structure methods, such as complete active space self-consistent field (CASSCF) calculations.[15]

Table 1. The equivalence coefficients for the low-energy terms of late Ln(III) ions.[6]

Ln(III)	Term	θ_2	θ_4	θ_6
Eu	$^7F_0$	0	0	0
	$^7F_1$	-1/5	0	0
Tb	$^7F_6$	-1/99	2/(11×1485)	-1/(13×33×2079)
Dy	$^6H_{15/2}$	-2/(9×35)	-8/(11×45×273)	$4/(11^2\times13^2\times3^3\times7)$
Ho	$^5I_8$	-1/(30×15)	-1/(11×10×273)	$-5/(11^2\times13^2\times3^3\times7)$
Er	$^4I_{15/2}$	4/(45×35)	2/(11×15×273)	$8/(11^2\times13^2\times3^3\times7)$
Tm	$^3H_6$	1/99	8/(3×11×1485)	-5/(13×33×2079)
Yb	$^2F_{7/2}$	2/63	-2/(77×15)	4/(13×33×63)

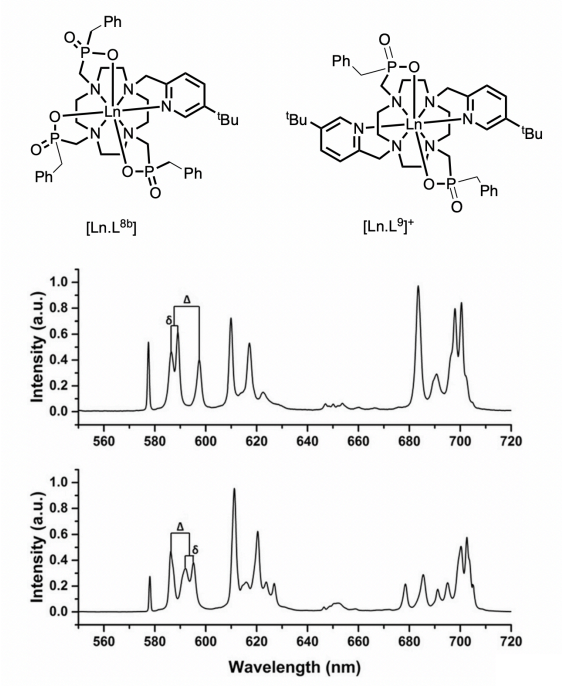

Figure 2. Europium emission spectra (295K, MeOH, λ_{exc} 270 nm of [EuL[8b]] (lower) and $[EuL^{9}]^{+}$ (upper) highlighting different splittings of the $\Delta J = 1$ manifold for $^5D_0 \rightarrow {}^7F_1$; in the spherical operator formalism $\Delta = -\frac{3}{10}B_0^2$, $\delta = -\frac{\sqrt{6}}{5}B_2^2$. [15,16]

Because the emissive state $^5D_0$ is non-degenerate, the splitting of the transition must arise from the ligand field splitting of the $^7F_1$ multiplet (excluding vibrational effects). Since J = 1, the series in Eq (1) terminates at k = 2, and when the complex has symmetry higher than C_2 only B_0^2 is non-zero and the spectrum exhibits two bands corresponding to the degenerate $m_J = \pm 1$ pair and the $m_J = 0$ singlet, whose separation is $\propto B_0^2$. In lower symmetry, the degeneracy of the $m_J = \pm 1$ states is lifted and $B_{\pm 2}^2$ is non-zero. Therefore, the $^5D_0 \rightarrow {}^7F_1$ band can be modelled with band-specific B_0^2 and B_2^2, which may differ slightly from the parameters determined by fitting all observable bands.[14,16] The splittings are given as $\Delta = 3\theta_2 B_0^2$ and $\delta = 2\theta_2 B_2^2$, and $\theta_2 = -1/5$ (Table 1), where ligand field parameters are defined for Stevens operators, and the renormalisation for more commonly used spherical tensors is given in the Figure 2 caption.[13] The sign of Δ is positive if the $m_J = 0$ component of $^7F_1$ is lower in energy than the barycenter of $m_J = \pm 1$ components, giving a singlet transition at higher energy than the doublet. Comparing the aza-phosphinate complexes [EuL[8b]] and $[EuL^{9}]^{+}$, (Figure 2), there is a change in the sign of B_0^2, which is positive for the latter. The sign of these crystal field parameters is tightly linked to the local symmetry at the Eu(III) ion. [12,14,17,18] Even though, B_q^k parameters determined for Eu(III) complexes can be very similar to isostructural complexes of other lanthanide ions, B_q^k depends on the radial part of the *f*-electron wavefunction which changes with nuclear charge, and

small changes in bond lengths and angles may also affect the angular part of B_q^k unexpectedly.

When the ligand field splitting is comparable with the splitting between spin-orbit multiplets, *J* is no longer a good quantum number, and the coupling scheme breaks down *e.g.* for Sm(III),[19] leading to the phenomenon of "*J* mixing", commonly invoked to explain unusual oscillator strengths and odd transitions in polarised emission spectra. [20-22] Despite this, many other spectral phenomena defy explanation, and "*J* mixing" is often cited as a 'catch-all', highlighting limitations in current understanding.[12,14,23]

Lanthanide magnetic moments,[24] which are often assumed to be independent of coordination environment [25,26] also routinely show reductions in room-temperature susceptibility values compared to the free-ion due to the ligand field effect; a notable 11% reduction was found for Ho(III).[27] Apart from the reduction of the average magnetic susceptibility, the ligand field also induces magnetic anisotropy that is the origin of paramagnetic NMR shifts and dramatically alters nuclear spin relaxation.

OVERVIEW OF FACTORS DETERMINING LIGAND FIELD SPLITTING

The spectral behaviour of several series of macrocyclic lanthanide(III) complexes [LnL^{1-9}] has been studied, owing to their interest as emissive probes in optical spectroscopy and microscopy,[28-30] or contrast agents in magnetic resonance imaging.[13,17,18]

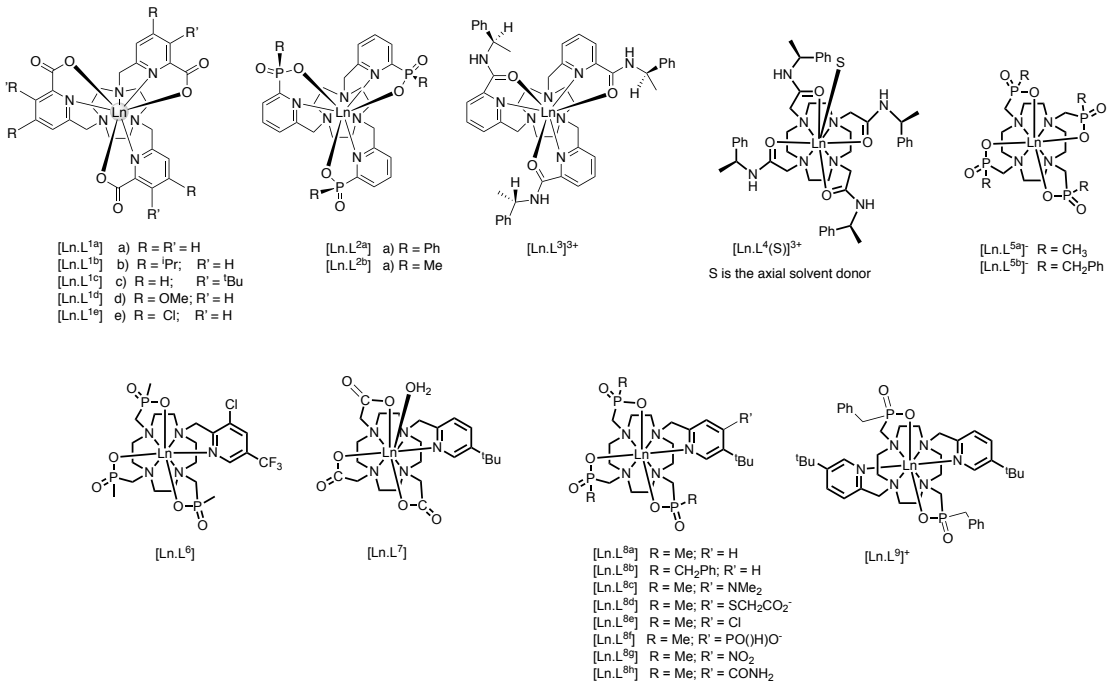

Chart 1

Design of complexes with desired optical and magnetic properties requires an understanding of correlations between molecular structure and the electromagnetic susceptibility tensors.[31] These correlations are often assumed to follow simple models. However, Judd-Ofelt-Mason theory fails to offer guidelines for the design of emissive lanthanide optical probes,[32-34] and similarly Bleaney's theory of magnetic anisotropy[11,35,36] has been widely used for NMR spectral fitting, but provides no guidance for paramagnetic shift reagent design.[37,38]

Examination of the emission spectral properties of the [LnL$^{1\text{-}9}$] series permits a dissection of the key factors determining the most important contribution to the ligand field. The size and sign of B_0^2 varies widely across these series of complexes, (Chart 1 and Table 2).

Table 2. Values of second order crystal field terms for Eu(III) complexes (from emission spectra at 295K in H_2O). Ligand field parameter values quoted in the spherical tensor formalism.

Complex	B_0^2 /cm^{-1}	B_2^2/ cm^{-1}
[EuL^{1a}]	< -200 [c]	0
[EuL^{2a}]	< +200 [c]	0
[EuL^{3}]$^{3+}$	+230 [c]	0
[EuL^{4}(H_2O)]$^{3+}$	-470 [a]	0
[EuL^{5a}]$^{-}$	-700	0
[EuL^{5b}]$^{-}$	-650	0
[EuL^{6}]	-550	-145
[EuL^{7}]	-455	-120
[EuL^{8a}]	-660	-122
[EuL^{8b}]	-650	-80
[EuL^{9}]$^{+}$	+735[b]	-220[b]

(a) with different axial donors, values changed dramatically, e.g. MeCN (-630); DMF (-340); DMSO (-150); HMPA(-85) and with fluoride replacing the coordinated water molecule, B_0^2 has a positive sign

(b) in methanol, values were +920 and -153 cm^{-1}

(c) data recorded in methanol, not water, where values are smaller; the value for [EuL^{2a}] represents an upper limit, owing to the lack of spectral resolution.

Variation of complex constitution and symmetry

i) In the series of C_3-symmetric complexes, [EuL$^{1\text{-}3}$], the triacetate, triphosphinate and triamide ligands gave values for B_0^2: [EuL^2] = [EuL^1] < [Eu.L^3]$^{3+}$. The sign is negative for [EuL^1], but positive for the other two in methanol.[39] The polarisability of the oxygen donor atoms can be hypothesised to determine the multipolar ion-oxygen interaction energy.

ii) In the series of square antiprismatic complexes, [Ln.L^4(S)]$^{3+}$, the axial donor, S, can be permuted.[40-43] When S is MeCN, B_0^2 = -630 cm^{-1} and replacement of MeCN by a more polarisable oxygen donor is energetically favourable in the sequence : H_2O < DMF < DMSO < HMPA (B_0^2: -470 < -340 < -150 < -85 cm^{-1}), correlating with the dipole moment change.[44] When the axial donor is replaced by fluoride, B_0^2 inverts sign causing a large change in magnetic susceptibility anisotropy, as the order of the m_J sublevels switches.[31] The importance of the 'axial component' of the ligand field was highlighted by Di Bari,[45] examining spectral behaviour of [Yb.L^5]$^-$ complexes. Another example of switching sign in B_0^2 for Yb(III) complexes, combined NMR, EPR and computational studies to track changes in the anisotropy of the magnetic susceptibility tensor.[46]

iii) For [Eu.L$^{1a\text{-}e}$] (Chart 1), B_0^2 changes as the *para* substituent in the pyridine ring varies. A linear correlation between the Hammett parameter, σ_p, and B_0^2 (R^2 = 0.97, in acetonitrile), is consistent with the strongly dipolar nature of the Ln–N_{py} interaction.[46] The variation of overall ligand polarizability and its directionality, involving the electrostatic interaction between induced dipoles on the ligand and the quadrupole moment on the Ln^{3+} ion, is important in determining the 'allowedness' of *f-f*

electronic transitions.[47,48] Thus, it is the *overall* ligand molecular polarisability that is important in determining the ligand field.

iv) Other examples of switches in the sign of B_0^2 can be identified, when complex constitution and local symmetry vary. The difference between the emission spectra of [EuL^{8b}] and [EuL^{9}]$^{+}$, (Figure 2), is consistent with a change in sign, as symmetry changes from C_1 to C_2.[3,14] Other cases have been reported, including systems involving reversible coordination of a polarizable N atom, which is replaced following protonation by water.[49-51]

Polyhedral distortion

In point-charge ligand field theory, the geometric position and charge of each atom determine contributions to the ligand field potential. An axial anionic donor gives a positive contribution to B_0^2, which becomes negative if in an equatorial position (switching at the "magic angle" $\theta \sim 54.7°$ or 125.3°),[52-55] leading to sensitivity of the ligand field potential to polyhedral distortion. The tricapped trigonal prismatic geometry is particularly sensitive, as noted by Binnemans, if all nine ligands are equivalent, and the two sets of axial donors have polar angles 45° and 135°, leading to exact cancellation of all contributions and hence $B_0^2 = 0$.[56]

The situation with [Ln.L$^{1-3}$] is different. The first coordination sphere has three sets of donors: nitrogen atoms from the macrocycle (N_{ax}) lie in axial positions (polar angle $\theta \sim 142°$); pyridyl N atoms in equatorial positions (N_{eq}, $\theta \sim 90°$); carboxylate oxygens in axial sites, ($\theta \sim 50°$). [2] In [LnL^{1a}], the two sets of N donors (N_{ax}, N_{eq}) give contributions to B_0^2 of similar magnitude but opposite sign and cancel out; this is because the opposite of a ligand in an axial position is a ring of donors in the equatorial plane, and here the three-fold equatorial disposition of N_{eq} balances the N_{ax}

contribution. However, the oxygen donors lie close to the magic angle and thus the ligand field is almost entirely ascribed to the oxygen atoms, resulting in an exquisite sensitivity of ligand field and magnetic anisotropy to very small variations in their *angular* position (Figure 3).[2] Emission studies with [EuL[1a]] showed a pronounced dependence of B_0^2 on solvent, suggesting that hydrogen bonding interactions with the oxygen donors could alter their effective polar angle θ. Indeed, the X-ray structure of [YbL[1b]] shows hydrogen bonding of water to the coordinated carboxylate oxygen, demonstrating this 'tugging' on the donor oxygen. For [YbL[1b]], [YbL[1e]] and [EuL[1e]] both carbonyl and carboxylate oxygen atoms served as hydrogen bond acceptors to the water hydrogen atom.[46]

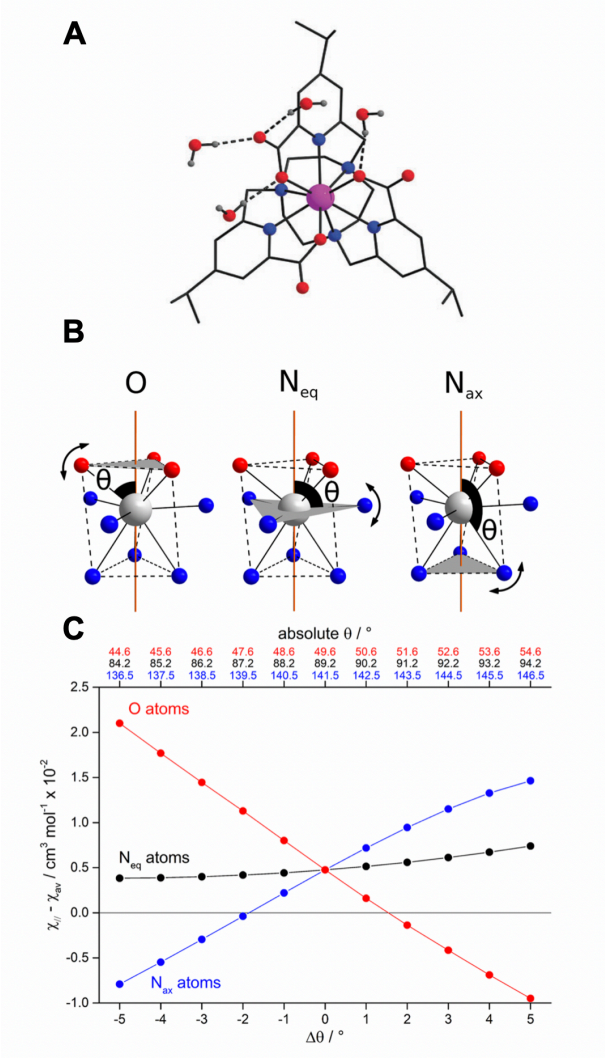

Figure 3. A) X-ray crystal structure of [YbL[1b]], showing hydrogen bonding of water, tugging at the ligand oxygen atoms. B) Schematic representation of the change in the polar angles θ for the oxygen, N_{eq} (py) and N_{ax} (ring) donor atoms in [DyL[1a]]. C) Calculated room temperature magnetic susceptibility anisotropy arising from distortion, where $\Delta\theta$ is the deviation from the lowest energy structure.[2]

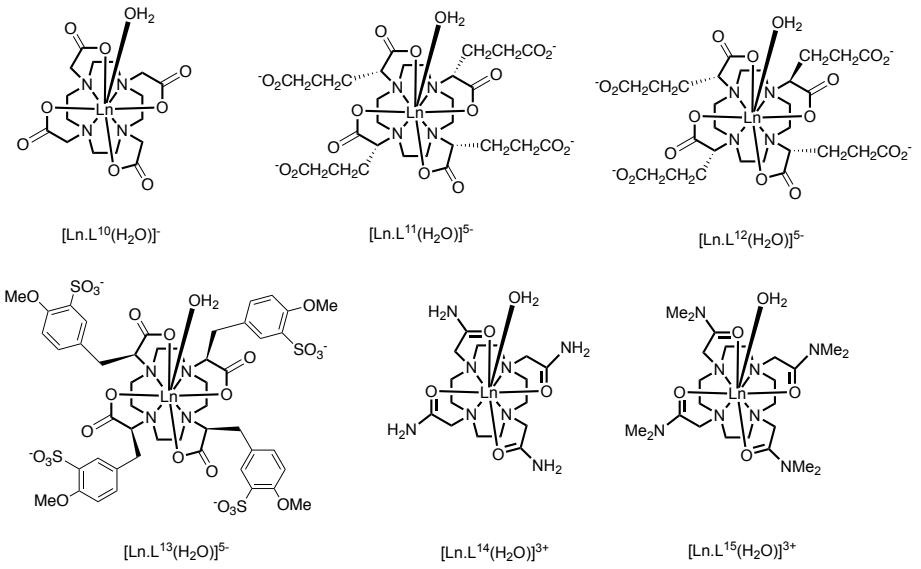

Chart 2

Table 3. Values of B_0^2 (spherical tensor formalism) determined by emission analysis for [EuL[10-15](OH$_2$)]

	B_0^2/ cm^{-1}	
Complex	SAP isomer	TSAP isomer
[EuL[10]]	-630	-400
(*RRRR*) – [EuL[11]]$^{5-}$	-760	-425
(*RRRS*) – [EuL[12]]$^{5-}$	-780	-445

(*SSSS*) – [EuL^{13}]$^{5-}$	-700	-410
[EuL^{14}]$^{3+}$	-475	-205
[EuL^{15}]$^{3+}$	-450	-185

In 9-coordinate lanthanide complexes based on 12-N_4 (*e.g.* DOTA[18]), the most common geometries are a mono-capped square antiprism (SAP) and a twisted version (TSAP). The twist angle between upper and lower planes of four donor atoms found in X-ray analyses vary around 40° and 25°, respectively. Values of B_0^2 for [EuL$^{10\text{-}15}$(OH$_2$)], (Chart 2, **Table 3**), show larger parameters in the SAP series.[40-44,57] These variations relate to polyhedral distortion, but may also be ascribed to changes in the axial water distances that are systematically longer (< 0.3 Å) in the TSAP series due to increased steric demand. Such behavior is consistent with the concept of non-integral metal ion hydration states, reducing in value between unity (Eu) and zero (Yb), through certain TSAP series, as the bond length to the water oxygen increases.[40-43,58]

Supramolecular effects: solvation and the degree of aggregation

The nature of the solvent and the state of complex aggregation are supramolecular effects. For [EuL^{1b}] and [EuL^{1a}] where no solvent is bound, emission spectra change significantly with solvent, highlighted in the $\Delta J = 1$ manifold (

Figure 4).[46] The variation can be attributed to differing time-averaged orientations of solvent dipoles, perturbing the Ln-O and Ln-N_{py} dipolar and quadrupolar interactions, consistent with solvent multipolar effects.[47,48,59-61] DOSY NMR studies of the diamagnetic analogue [YL^{1b}] revealed clear evidence for aggregation that was

greatest in chloroform and was positively correlated with the ligand field splitting.[62] With [YL[1a]], in water only the monomer was evident, whereas in CD_3CO_2D and CF_3CO_2D the aggregation state was 4 to 5.

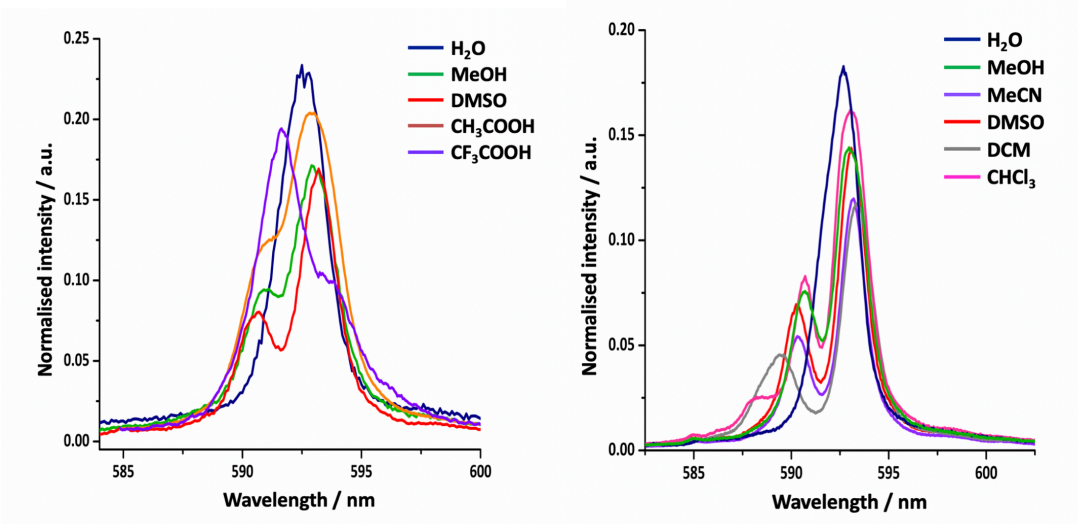

Figure 4. (*left*) The $\Delta J = 1$ manifold for [EuL[1a]] in the stated solvents revealing the sign change of B_0^2 in CF_3CO_2H. (*right*) Related emission spectra for [EuL[1b]] in the given solvents (298 K, λ_{exc} = 268 nm).[46,62]

In summary, ligand field splitting of lanthanide complexes is a sensitive function of several factors: the nature and polarizability of the ligand and its donors; the type and degree of polyhedral distortion; the presence and extent of solvent dipolar interactions; hydrogen bonding effects and the degree of supramolecular order. Each factor may be non-negligible in defining the ligand field, and their relative importance varies for different lanthanides.

PSEUDOCONTACT SHIFT AND BLEANEY'S THEORY OF MAGNETIC ANISOTROPY

When a lanthanide is treated as a point with second-rank magnetic susceptibility and infinitely fast magnetic relaxation, an additional isotropic shielding experienced by nearby nuclei is given by: [63]

$$\delta^{PCS} = \frac{1}{12\pi r^3}\left[\chi_{ax}\left(3\cos^2\theta - 1\right) + 3\chi_{rh}\sin^2\theta\cos 2\varphi\right] \quad (2)$$

where θ, ϕ, r are nuclear coordinates in the eigenframe of the magnetic susceptibility tensor. The eigenvalues of the traceless susceptibility tensor are labelled to satisfy the relation $|\chi_x|<|\chi_y|<|\chi_z|$, with axiality $\chi_{ax} = 3\chi_z/2$ and rhombicity $\chi_{rh} = (\chi_x-\chi_y)/2$. Below we also use terms of $\chi_{av} = Tr(\boldsymbol{\chi})/3$ and $\chi_{\parallel} = \chi_z + \chi_{av}$.

Bleaney's theory of magnetic anisotropy[11,35,36,64] shows that for a well-isolated J multiplet in the high temperature approximation, the anisotropy of the susceptibility tensor depends only on the second rank B_0^2 and B_2^2 ligand field parameters:

$$\chi_{ax} = -\frac{\mu_0\mu_B^2 C_J B_2^0}{10\left(kT\right)^2}; \quad \chi_{rh} = -\frac{\mu_0\mu_B^2 C_J B_2^2}{30\left(kT\right)^2} \quad (3)$$

where C_J is Bleaney's constant, defined for each lanthanide(III) ion (C_J = –158 (Tb), –181 (Dy), –71.2 (Ho), +58.8 (Er), +95.3 (Tm), and +39.2 (Yb)), and μ_B is the Bohr magneton.

Approximations and their limits

Assuming that the ligand field parameters do not vary between lanthanide ions, Eq. (3) suggests that χ_{ax}/χ_{rh} remains constant within the series and PCS only varies due to the change in the value of C_J. However, if the overall ligand field splitting is *greater* than kT (**Figure 5**),[28,63,64] the Bleaney formula is no longer valid, and χ_{ax}/χ_{rh} and the

eigenframe of the susceptibility tensor will depend on temperature.[66] It is evident from low temperature measurements of $[LnL^{10}](H_2O)]^-$ that the principal axis changes direction by up to 90 degrees from Tb to Yb.[67,68 69]

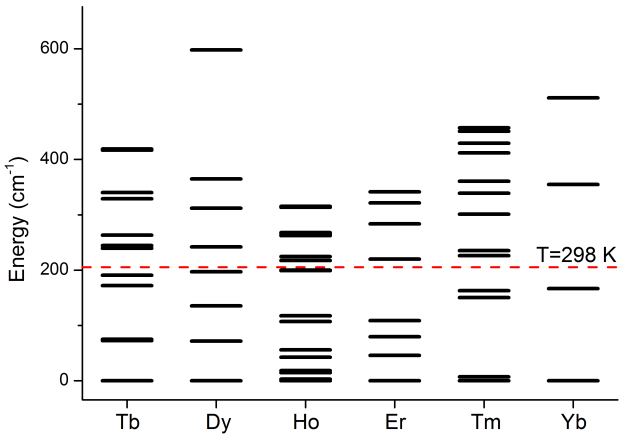

Figure 5. Energy splitting of the ground terms of $[LnL^{8a}]$ due to the ligand field, computed with CASSCF-SO in MOLCAS 8.0.[1]

Wavefunction calculations accounting for orbital degeneracy and correlation amongst the 4*f* electrons, as well as spin-orbit coupling (CASSCF-SO method) are used to determine ligand field splittings in lanthanide complexes.[70,71] Such calculations, (*e.g.* for $[LnL^{8a}]$, **Figure 5**), clearly show that in all cases the splitting is larger than kT. Thus, if Eqs (2) and (3) are used to determine B_0^2 and B_2^2 from PCS data, the parameters may appear to be very different for each lanthanide simply because Bleaney's approximations do not hold.[72]

Equation (2) also assumes a point magnetic source at the nuclear position of the lanthanide ion; a revised approach has recently emerged where the distribution of 4*f* electron density can be accounted for.[73] There are two distinct reasons for such a distribution to occur: (i) spin delocalisation and (ii) fast tag mobility. Disregarding the

nature of the distribution, the mathematical formulation is the same. The effect of spin delocalisation across ligands can be easily accounted for by *ab initio* calculation of the dipolar hyperfine tensors, but the tag mobility is often ignored despite the possible ~30% deviation from a point model for nuclei close to the tag.[74]

Contact contribution to paramagnetic shift

In most of the cases considered in this review, the proton contact shift is negligible compared to the PCS, and the point-dipole approximation in Eq. (2) is valid. The contact shift is proportional to the isotropic hyperfine coupling (itself related to spin density at the nucleus) and the isotropic magnetic moment of the lanthanide ion. Accounting for admixture of excited states with different J to the ground term, the isotropic magnetic moment can be corrected,[75] and the ratio of contact contribution to the PCS can be estimated for different lanthanides provided that all other parameters in the series stay the same.[76] Such estimations suggest that in the Tb-Yb series the most pronounced effect of a contact contribution is expected for Ho/Er.

NMR SHIFT BEHAVIOUR OF SYSTEMS WITH LARGE MAGNETIC ANISOTROPY

Detailed analyses of PCS data have been undertaken for isostructural complexes, with known solution speciation.[28,38,77-81] A semi-automated combinatorial assignment procedure using PCS data, XRD structure and NMR relaxation rates to limit the combinatorial space (in Spinach[82]) was deployed for [LnL^{8a}], enabling assignment of almost every proton resonance.[1] Subsequently, the traceless part of the magnetic susceptibility tensor was obtained by fitting Eq.(2) to experimental data, giving excellent agreement ($R^2 > 0.99$).

The experimentally determined susceptibility tensor can be displayed as a PCS field (Figure 6), revealing significant variations in the amplitude, shape and orientation for the [LnL^{8a}] series. Bleaney's theory predicts only the amplitude and sign should vary. However, the tensors change from almost fully rhombic (Dy and Tb; PCS field resembles d_{xz} orbital) to near axial (Tm, PCS field resembles d_z^2 orbital). Critically the *tilt angle* β of the main anisotropy axis, relative to the molecular pseudo-symmetry axis, varies significantly between complexes: Tb 8°; Dy 20°; Ho 22°; Er 8°; Tm 6°; Yb 23°.

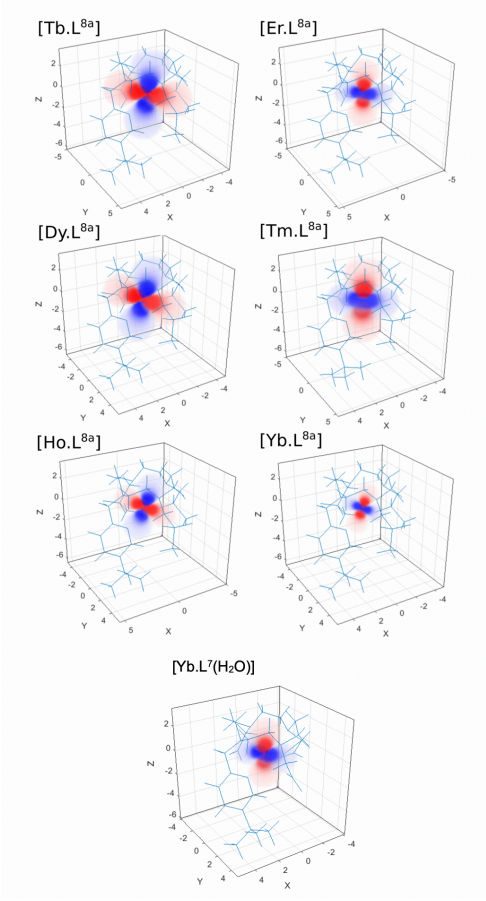

Figure 6. Pseudocontact shift fields for [LnL^{8a}], reconstructed using Spinach[81] with the 'best-fit' magnetic susceptibility tensor. Positive PCS red; negative blue. Note changes in the orientation, size and tilt of fields between [LnL^{8a}] complexes[1] and how the change in coordination in [YbL^7(H$_2$O)] vs. [YbL^{8a}] affects the PCS field.[83]

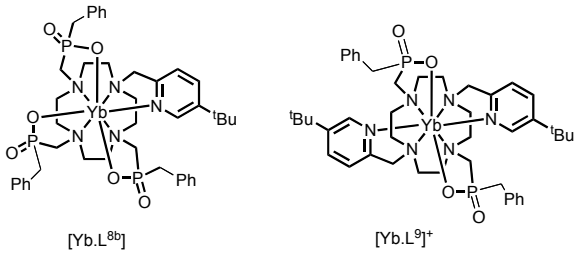

Chart 3

To illustrate the sensitivity of magnetic susceptibility anisotropy to structural change, consider PCS shifts for [YbL^{8b}] and [YbL^{9}]$^{+}$(Chart 3). The ^{t}Bu NMR chemical shifts vary markedly across the series but appear in the same order, notwithstanding the B_0^2 sign inversion (Figure 7 and Figure 2);[3] Bleaney's theory predicts the shift sense should be inverted.

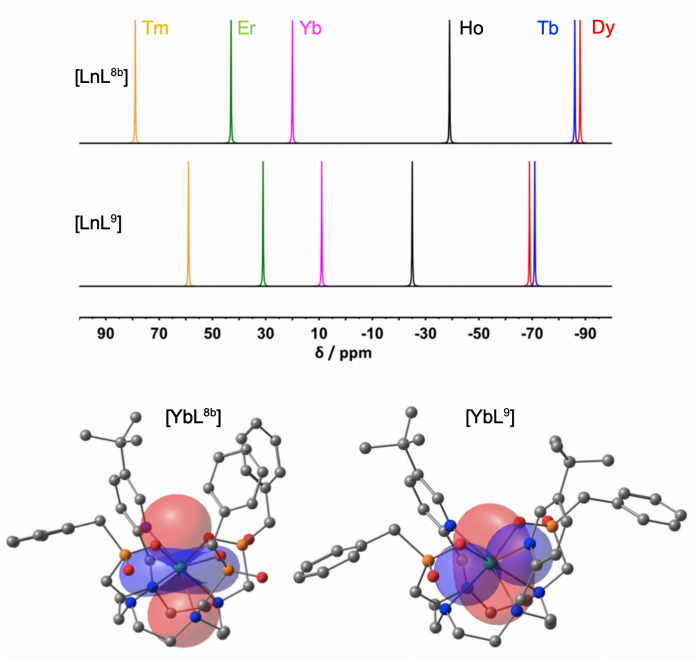

Figure 7. (*top*) Schematic representation of ^{t}Bu NMR shifts: [LnL^{8b}] (*upper*), [LnL^{9}]Cl (*lower*) (CD_3OD, 11.7 T, 295 K) (yellow Tm; green Er; magenta Yb; black Ho; red Dy; blue Tb); (*bottom*) Pseudocontact shift fields, for [YbL^{8b}] (*left*), [YbL^{9}]$^{+}$ (*right*). Positive PCS red (+200 ppm), negative blue (-200 ppm). Twist angles of each TSAP complex were 26.4° and 18.5°, i.e. greater distortion in the cationic complex.[3]

The explanation lies in the magnetic susceptibility tensors, expressed in their very different PCS shift fields. While the second-order magnetic anisotropy changes sign, the negative PCS lobe is still oriented in the "equatorial plane", because along with the change in sign of B_0^2, there is a 90° rotation in orientation of the principal magnetic axis. Thus, the combined effect of the change in sign *and* orientation of the ligand field were shown to give rise to similar PCS fields for the ^{t}Bu protons, explaining the 'hidden' changes in PCS behaviour.[3]

NMR SHIFT BEHAVIOUR OF SYSTEMS WITH SMALL LIGAND FIELD SPLITTINGS

Complexes ([LnL$^{1-3}$]) adopt tricapped trigonal prismatic structures and possess small ligand field splittings close to *kT*. Yet, their PCS values do not conform to Bleaney's theory.[31,37,38] Both the sign and magnitude of their ligand field parameters are sensitive to local polarity changes and polyhedral distortion. They are particularly sensitive to perturbation of the polar angle of oxygen donor atoms, θ, defining the angle subtended by the Ln–O vector compared to the C_3 axis. As θ lies close to the 'magic' angle, small variations cause major changes in magnetic susceptibility anisotropy.[2,46]

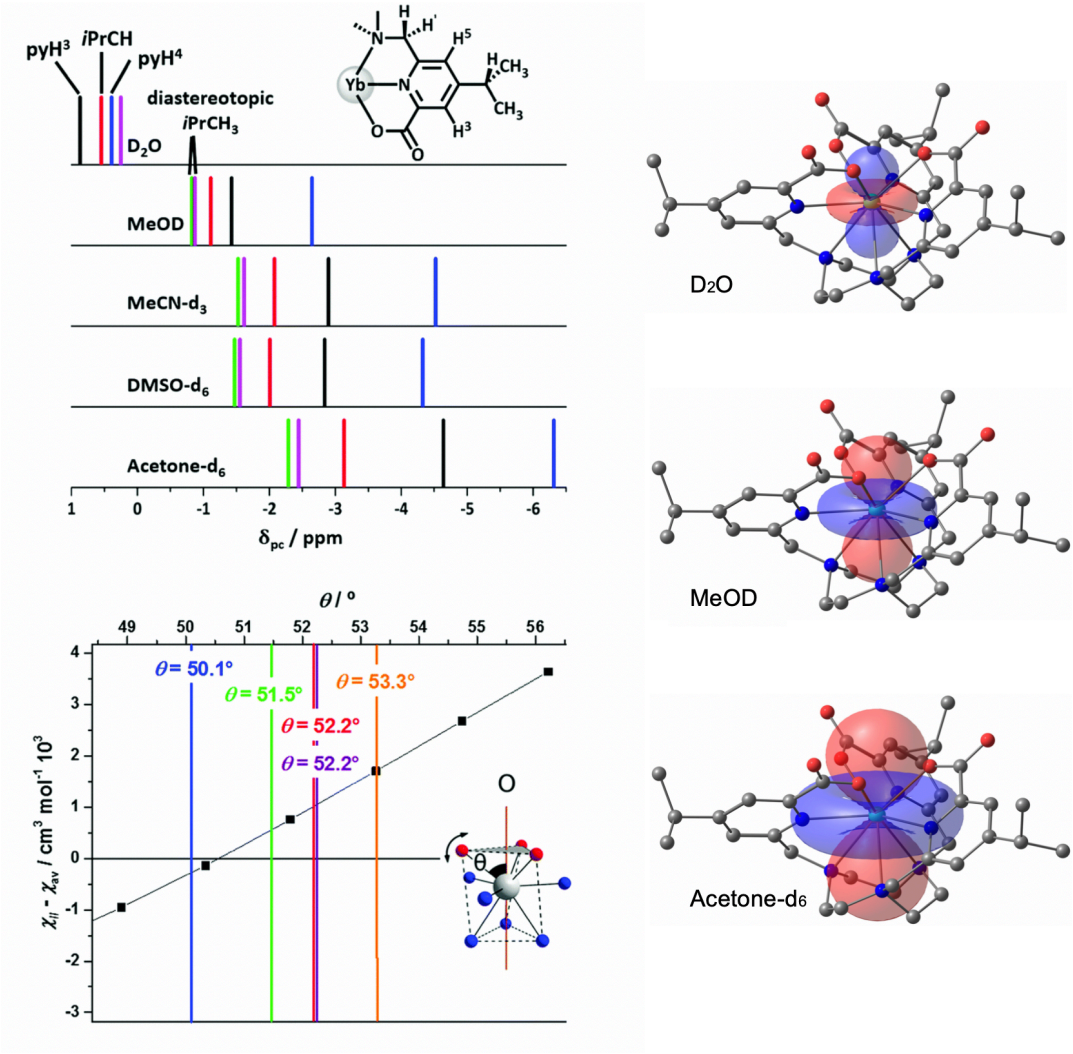

Figure 8 (left) Schematic representation of PCS (295 K, 4.7 T) for pyridyl H^3, H^5, ^{i}Pr resonances of [YbL^{1b}], and variation in the susceptibility anisotropy with θ : D_2O (*blue*); CD_3OD(*green*), CD_3CN (*purple*), DMSO-d^6 (*red*) , acetone-d^6 (*orange*); diastereotopic methyl resonances are isochronous in D_2O; (*right*) PCS fields for [YbL^{1b}], (using Spinach[82]): positive PCS red; negative blue. [46]

For [YbL^{1b}], DFT was used to determine a pseudo-solution structure with imposed C_3 symmetry and CASSCF-SO calculations gave the anisotropy of the susceptibility tensor (squares, Figure 8). The experimental values of $\chi_{\parallel} - \chi_{av}$ were determined

assuming a fixed structural model based on experimental PCS, referenced to the diamagnetic Y(III) complex. A comparison was then made with the CASSCF-SO-calculated susceptibility anisotropy, to determine the 'spectroscopic' average value of θ in solution. In [YbL^{1b}] the diastereotopic methyl groups of the isopropyl substituent serve as a local probe of magnetic anisotropy. The PCS fields in acetone, water and methanol highlight the sensitivity to solvent. The PCS field changes sign as the magnetic susceptibility anisotropy switches from 'easy axis' to 'easy plane' in D_2O.[46] Similar solvent dependences were found for [LnL^{1a}] (Dy, Er, Eu).[2]

The sensitivity of magnetic anisotropy in these lanthanide complexes with small ligand field splittings was shown to have a major impact on solid-state EPR behaviour.[84] The magnetic and spectroscopic properties depend upon a number of factors that cannot be disentangled: a distribution of structural parameters generates a range of B_0^2 values; an electronic structure sensitive to thermal changes of the ligand structure; thermally accessible EPR-active excited states; disordered solvation influencing the local ligand field. Each effect is present across the [LnL$^{1-3}$] series, making interpretation of EPR spectra very difficult for systems with small magnetic anisotropy.[84]

NMR SHIFT BEHAVIOUR OF MOBILE LANTHANIDE TAGS ON PROTEINS

Complexes with large magnetic anisotropies are often used as tags in protein NMR to provide structural constraints,[85,86] where large magnetic anisotropy is preferred so that PCS is measurable even at distances of 40 Å. The tag is often attached by a flexible

linker, but mobility results in big deviations from the point-dipole approximation, at <15 Å.

A generalization of McConnell's expression, Eq. (4), was derived for lanthanide tag mobility in protein NMR: [73,74,87]

$$\delta(\mathbf{r}) = -\frac{1}{3}\frac{\vec{\nabla}^{\mathrm{T}} \cdot \boldsymbol{\chi}_{\mathrm{t}} \cdot \vec{\nabla}}{\vec{\nabla}^{\mathrm{T}} \cdot \vec{\nabla}} \rho(\mathbf{r}) \qquad (4)$$

where $\vec{\nabla}$ is the gradient operator, $\rho(\mathbf{r})$ the probability distribution of the spatial position of the lanthanide tag, subscript t indicates the traceless part of the magnetic susceptibility tensor. The susceptibility is assumed to be the same in every point of the probability density.[74] The latter assumption may be lifted, but the corresponding equation is considerably harder to solve. The partial differential equation (4) can be solved using three-dimensional Fourier transforms:[74]

$$\delta(\mathbf{r}) = -\frac{1}{3}\mathrm{Re}\left[\mathrm{FFT}_{-}\left\{\frac{\vec{k}^{\mathrm{T}} \cdot \boldsymbol{\chi}_{\mathrm{t}} \cdot \vec{k}}{\vec{k}^{\mathrm{T}} \cdot \vec{k}} \mathrm{FFT}_{+}\left\{\rho(\mathbf{r})\right\}\right\}\right] \qquad (5)$$

where FFT_{+} refers to the forward fast-Fourier Transform and FFT- inverse. If the probability density is defined on a grid, numerical solution of eq. (5) gives the PCS values. The solution of the inverse problem is possible; one can extract probability density from PCS data. Numerical solvers for both direct and inverse problems are available.[82] The resulting lanthanide probability densities from PCS are in agreement with Double Electron-Electron Resonance (DEER) spectroscopy, and PCS fits are significantly improved near the tag, (Figure 9).[87]

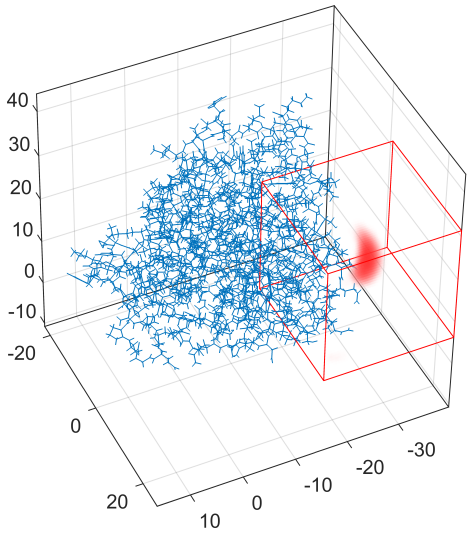

Figure 9 Tm^{3+} ion distribution (*red*) in a DOTA-M8 tagged S50C mutant of human carbonic anhydrase II (*blue*), extracted from PCS data. The red cube indicates the volume where the probability density can vary during fitting. The source code is available in Spinach;[82] axes in Å.

LANTHANIDE RELAXATION AND ITS ANISOTROPY

Common MRI contrast agents contain magnetically isotropic Gd^{3+} ions. Their long electron relaxation times mean that PCS is absent, and the effect is only to accelerate nuclear relaxation.[88] Likewise, relaxation enhancement experiments in NMR often use magnetically isotropic Mn^{2+} or Gd^{3+} complexes to maximise the volume affected by the metal and minimise PCS.[89] Following nuclear relaxation enhancement models designed for these ions, it has often been assumed that the enhancements show a simple $1/r^6$ dependence on the electron-nuclear distance, without angular terms in the molecular frame of reference.

Nuclear relaxation enhancement by unpaired *f* electrons of lanthanide complexes has two principal components. One ("dipolar relaxation") comes from stochastic modulation of the electron-nuclear dipolar interaction, the other ("Curie relaxation")

from rotational modulation of extra nuclear shielding caused by the presence of the unpaired electron. The angular dependence in non-Gd lanthanides[4] was first acknowledged for Curie relaxation.[90] The reasons are twofold. Firstly, magnetic susceptibility tensor anisotropy can be as large as the isotropic part, contradicting the assumption made by Gueron when he derived Curie relaxation theory.[91] Secondly, zero field splitting can be much stronger than the electron Zeeman interaction – the opposite limit from the classical Solomon-Bloembergen-Morgan theory of lanthanide-induced dipolar relaxation.[92]

Experimental proof came from relaxation rate measurements in complexes where all nuclei in the ligand cages could be unambiguously assigned, and atomic coordinate estimates were available from DFT calculations,[28,377,38,93-95] (**Chart 1** and Figure 10).

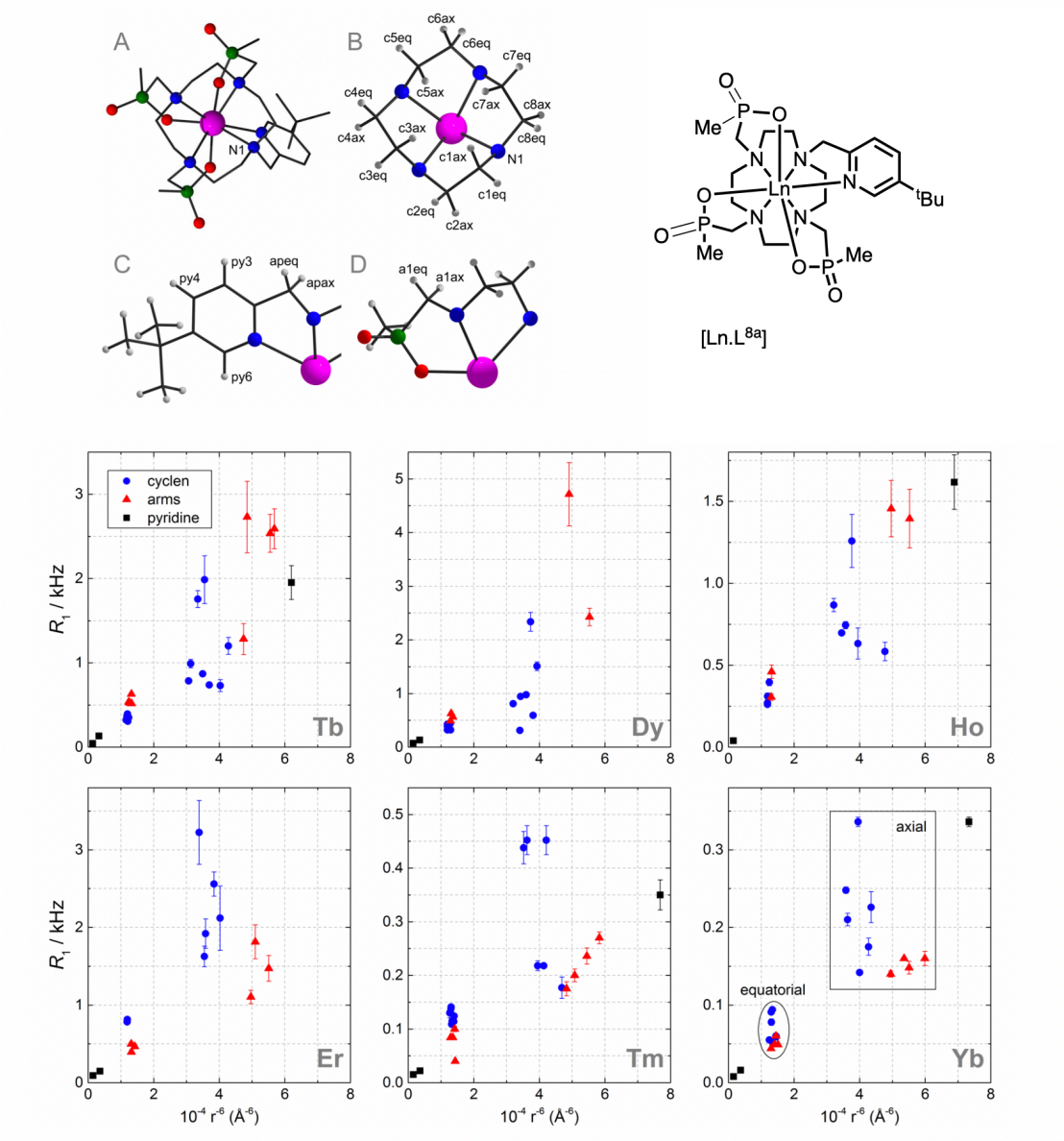

Figure 10 Longitudinal relaxation rates in [LnL^{8a}] complexes as functions of Ln–H distance (r^{-6}, D_2O 295K, 1 Tesla), for 12-N_4 ring protons (blue circles), ligand arms (red triangles), pyridine protons (black squares). In the Yb set, axial and equatorial protons are indicated. A pure r^{-6} dependence is a straight line. [4]

It is obvious from Figure 10 that nuclear relaxation enhancements at low magnetic field (1 Tesla) *do not* depend simply on the distance to the lanthanide ion. The relaxation rates also appear to depend on the sign of the magnetic anisotropy: in complexes with easy-plane anisotropy (Tb, Dy, Ho), ligand arm protons relax faster than macrocyclic ring protons; the opposite is true for the complexes with easy-axis anisotropy (Er, Tm, Yb).

Encouraged by these findings, we updated the dipolar relaxation theory[4] to include the direction of the Ln-H vector in the molecular frame:

$$\begin{aligned} R_1^{\text{dip}} &= \frac{2}{3}\left(\frac{\mu_0}{4\pi}\right)^2 \frac{\gamma_{\text{N}}^2}{r^6}\text{Tr}\left[\left(3\hat{r}\cdot\hat{r}^{\text{T}}-\mathbf{1}\right)^2\mathbf{G}\left(\omega_{\text{N}}\right)\right] \\ R_2^{\text{dip}} &= \frac{1}{3}\left(\frac{\mu_0}{4\pi}\right)^2 \frac{\gamma_{\text{N}}^2}{r^6}\text{Tr}\left[\left(3\hat{r}\cdot\hat{r}^{\text{T}}-\mathbf{1}\right)^2\left(\mathbf{G}\left(0\right)+\mathbf{G}\left(\omega_{\text{N}}\right)\right)\right] \end{aligned} \tag{6}$$

$$\mathbf{G}\left(\omega\right) = \int_0^\infty \mathbf{G}\left(\tau\right) e^{-\tau/\tau_{\text{R}}} e^{-i\omega\tau} d\tau \tag{7}$$

Where the spectral power density $\mathbf{G}(\omega)$ is no longer a scalar, but a tensor accommodating stochastic dynamics of the electron spin as well as molecular rotation, and $\hat{r}$ is the unit vector pointing in the same direction as $\vec{r}$ – further details may be found in the paper cited above.

Similar observations were made at higher field 9.4 T for [Ln.L[8a]] complexes (Ln=Tb-Yb), where the Curie contribution dominates. For Curie relaxation it turned out to be essential to account for the antisymmetric component in the total nuclear shielding tensor

$$\boldsymbol{\sigma} = \boldsymbol{\sigma}_0 - \mathbf{D}\cdot\boldsymbol{\chi} \tag{8}$$

That includes diamagnetic shielding tensor $\boldsymbol{\sigma}_0$ and paramagnetic shielding tensor, which is proportional to dipolar matrix **D** and magnetic susceptibility tensor $\boldsymbol{\chi}$. This is

necessary because the antisymmetric part is significant here – the product of two symmetric matrices is only symmetric when they commute. With the relevant extra terms in place the Curie relaxation rates become:

$$\begin{aligned} R_1^{\text{Curie+CSA}} &= \frac{1}{2}\Lambda_{\boldsymbol{\sigma}}^2\omega_{\text{N}}^2\frac{\tau_{\text{R}}}{1+9\omega_{\text{N}}^2\tau_{\text{R}}^2}+\frac{2}{15}\Delta_{\boldsymbol{\sigma}}^2\omega_{\text{N}}^2\frac{\tau_{\text{R}}}{1+\omega_{\text{N}}^2\tau_{\text{R}}^2} \\ R_2^{\text{Curie+CSA}} &= \frac{1}{4}\Lambda_{\boldsymbol{\sigma}}^2\omega_{\text{N}}^2\frac{\tau_{\text{R}}}{1+9\omega_{\text{N}}^2\tau_{\text{R}}^2}+\frac{1}{45}\Delta_{\boldsymbol{\sigma}}^2\omega_{\text{N}}^2\left(4\tau_{\text{R}}+\frac{3\tau_{\text{R}}}{1+\omega_{\text{N}}^2\tau_{\text{R}}^2}\right) \end{aligned} \tag{9}$$

$$\Lambda_{\boldsymbol{\sigma}}^2=\left(\sigma_{\text{XY}}-\sigma_{\text{YX}}\right)^2+\left(\sigma_{\text{XZ}}-\sigma_{\text{ZX}}\right)^2+\left(\sigma_{\text{YZ}}-\sigma_{\text{ZY}}\right)^2$$

$$\begin{aligned} \Delta_{\boldsymbol{\sigma}}^2 &= \sigma_{\text{XX}}^2+\sigma_{\text{YY}}^2+\sigma_{\text{ZZ}}^2-\sigma_{\text{XX}}\sigma_{\text{YY}}-\sigma_{\text{XX}}\sigma_{\text{ZZ}}-\sigma_{\text{YY}}\sigma_{\text{ZZ}}+ \\ &+\frac{3}{4}\left[\left(\sigma_{\text{XY}}+\sigma_{\text{YX}}\right)^2+\left(\sigma_{\text{XZ}}+\sigma_{\text{ZX}}\right)^2+\left(\sigma_{\text{YZ}}+\sigma_{\text{ZY}}\right)^2\right] \end{aligned} \tag{10}$$

here, $\Lambda^2_{\boldsymbol{\sigma}}$ is the first and $\Delta^2_{\boldsymbol{\sigma}}$ the second rank invariant of the chemical shielding tensor. These equations have been incorporated into Spinach[82]; for [LnL[8a]], the modifications yielded a much better agreement with experiment (Figure 11). [4]

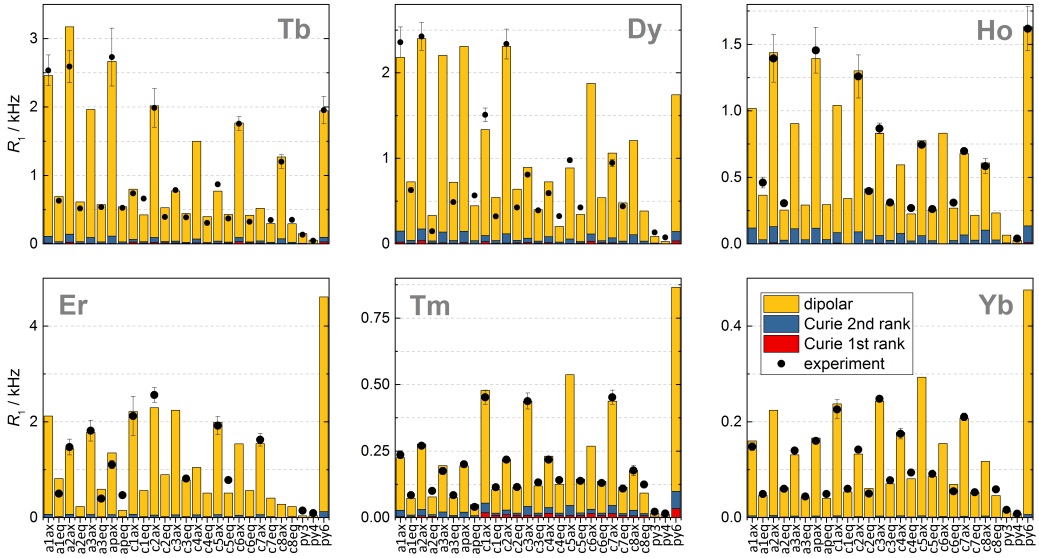

Figure 11 Experimental longitudinal relaxation rates (black dots), for the ligand cage nuclei of [Ln.L[8a]] in D_2O at 295 K and 1 Tesla. The calculated rates are shown as bars and colour-coded by the mechanism.[4]

In summary, the presence of magnetic anisotropy required a fundamental update of the relevant nuclear relaxation theories. These updates revealed strong molecular-frame angular dependencies in paramagnetic relaxation enhancements. In systems with large magnetic anisotropy and at short electron-nuclear distances the classical Solomon-Bloembergen-Morgan and Gueron expressions should not be used.

SUMMARY AND CONCLUSIONS

The ligand field for a lanthanide complex varies with the nature of the ligand, metal ion and its environment. The size and sign of ligand field parameters are difficult to determine experimentally, but information can be gained using optical spectroscopy with Eu(III) complexes.[9] They are sensitive to several factors including: the nature

and polarizability of the overall ligand and donor atoms; the type and degree of geometric distortion; the extent of solvent dipolar interactions; specific hydrogen bonding effects and the degree of supramolecular order.

Bleaney's magnetic anisotropy theory provided guidance in rationalising NMR PCS data. However, its crude approximations and limitations are apparent. In explaining the nature and magnitude of PCS data, both the ligand field splitting and the type, size *and* orientation of the principal component of the magnetic susceptibility tensor are key. The latter can be determined by careful magneto-structural correlations [27,31,2,46] assessed by VT magnetic susceptibility measurements, low temperature EPR studies and modern computational methods.

Considerable caution is needed using PCS data for structural refinement. Such methods are used in biomolecular analyses, but may fail when the lanthanide ion is permuted. Delving more deeply, the ordering, nature and relative Boltzmann population of the m_J sublevels for a given lanthanide ion complex is key to understanding the overall magnetic susceptibility and its directional dependences.

The nuclear relaxation induced by lanthanide ions can be anisotropic in the molecular frame, and accounting for this anisotropy can drastically improve agreement between experiment and theoretical models. Analyses based only on distance variations are a crude approximation for both dipolar and Curie relaxation mechanisms. Biomolecular structural refinement using lanthanide spin tags must account for this anisotropy or risk significant errors; any work using simple $1/r^6$ models for lanthanide labelled systems should be considered with appropriate caution.

BIOGRAPHICAL INFORMATION

David Parker, was born in Leadgate, England on 30th July 1956. Educated in the state sector, he read Chemistry at Oxford University (1974-78), and remained there to study with John Brown for a DPhil, which he gained in 1980. Following a NATO Fellowship in Strasbourg with Jean-Marie Lehn, he returned to the NE of England in early 1982 as a Lecturer in Chemistry at Durham University. He gained several national and international awards and prizes for work that embraces several aspects of contemporary chemistry, including the design of sensors, targeted imaging probes and therapeutic agents, as well as major contributions to chiral analysis and mechanistic studies. He is a Professor of Chemistry at Durham University.

Elizaveta Suturina studied physics at Novosibirsk State University where she obtained her undergraduate degree and DPhil in chemical physics working in the group of Nina Gritsan. She then moved to work in Max-Planck Institute with Frank Neese and Mihail Atanasov on *ab initio* modelling of molecular magnetic properties and then joined Ilya Kuprov' group to work on NMR theory and modelling of paramagnetic systems. In 2018, she was awarded Prize fellowship from the University of Bath where she is currently establishing her research group.

Ilya Kuprov is a magnetic resonance specialist and the leading author of Spinach - an advanced spin dynamics simulation package. He did his undergraduate degrees at Novosibirsk State University before moving to Oxford for a DPhil. He was a Lecturer at Durham University, and is presently an Associate Professor at Southampton. IK is

the Secretary of the Electron Spin Resonance Group of the Royal Society of Chemistry, and an Associate Editor at Science Advances. He has published about a hundred papers, principally on the theoretical and computational aspects of magnetic resonance spectroscopy and imaging.

Nicholas Chilton obtained his BSc Adv (Hons) in chemistry in the group of Prof. Keith Murray at Monash University, Australia, before moving to the UK in 2013 to undertake his PhD with Profs. Richard Winpenny and Eric McInnes at The University of Manchester. In 2016 he obtained a Ramsay Memorial Research Fellowship and started his own research group at The University of Manchester, followed by a Presidential Fellowship in 2018 and a Royal Society University Research Fellowship in 2019. He is currently a Senior Lecturer at The University of Manchester, and holds a number of prizes and awards.

Author Contributions

The manuscript was written through contributions of all authors. All authors have given approval to the final version of the manuscript.

ACKNOWLEDGMENTS

We thank EPSRC for grant support (EP/N007034/1, EP/N006909/1, EP/N006895/1) and talented colleagues in Manchester, Southampton Bath and Durham whose names appear below for their conscientiousness, resilience and excellence.

REFERENCES

(1) Suturina, E. A.; Mason, K.; Geraldes, C. F.; Kuprov, I.; Parker, D. Beyond Bleaney's Theory: Experimental and Theoretical Analysis of Periodic Trends in Lanthanide-Induced Chemical Shift. *Angewandte Chemie International Edition* **2017**, *56*, 12215-12218.

(2) Vonci, M.; Mason, K.; Suturina, E. A.; Frawley, A. T.; Worswick, S. G.; Kuprov, I.; Parker, D.; McInnes, E. J.; Chilton, N. F. Rationalization of Anomalous Pseudocontact Shifts and Their Solvent Dependence in a Series of C_3-Symmetric Lanthanide Complexes. *Journal of the American Chemical Society* **2017**, *139*, 14166-14172.

(3) Harnden, A. C.; Suturina, E. A.; Batsanov, A. S.; Senanayake, P. K.; Fox, M. A.; Mason, K.; Vonci, M.; McInnes, E. J.; Chilton, N. F.; Parker, D. Unravelling the Complexities of Pseudocontact Shift Analysis in Lanthanide Coordination Complexes of Differing Symmetry. *Angewandte Chemie International Edition* **2019**, *131*, 10396-10400.

(4) Suturina, E. A.; Mason, K.; Geraldes, C. F.; Chilton, N. F.; Parker, D.; Kuprov, I. Lanthanide-induced relaxation anisotropy. *Physical Chemistry Chemical Physics* **2018**, *20*, 17676-17686.

(5) Stevens, K. Matrix elements and operator equivalents connected with the magnetic properties of rare earth ions. *Proceedings of the Physical Society. Section A* **1952**, *65*, 209.

(6) Stevens, K. W. H. Matrix Elements and Operator Equivalents Connected with the Magnetic Properties of Rare Earth Ions. *Proceedings of the Physical Society. Section A* **1952**, *65*, 209-215.

(7) Mulak, J.; Gajek, Z.: *The effective crystal field potential*; Elsevier, 2000.

(8) Eyring, L.; Gschneidner, K. A.; Lander, G. H.: *Handbook on the physics and chemistry of rare earths*; Elsevier, 2002; Vol. 32.

(9) Wybourne, B. G.; Smentek, L.: *Optical spectroscopy of lanthanides: magnetic and hyperfine interactions*; CRC press, 2007.

(10) Bünzli, J.-C. G.; Eliseeva, S. V.: Basics of Lanthanide Photophysics. In *Lanthanide Luminescence: Photophysical, Analytical and Biological Aspects*; Hänninen, P., Härmä, H., Eds.; Springer Berlin Heidelberg: Berlin, Heidelberg, 2011; pp 1-45.

(11) Bleaney, B. Nuclear magnetic resonance shifts in solution due to lanthanide ions. *Journal of Magnetic Resonance (1969)* **1972**, *8*, 91-100.

(12) Binnemans, K.; Görller-Walrand, C. A simple model for crystal field splittings of the 7F1 and 5D1 energy levels of Eu3+. *Chemical Physics Letters* **1995**, *245*, 75-78.

(13) Finney, K. L. N.; Harnden, A. C.; Rogers, N. J.; Senanayake, P. K.; Blamire, A. M.; O'Hogain, D.; Parker, D. Simultaneous triple imaging with two PARASHIFT probes: encoding anatomical, pH and temperature information using

magnetic resonance shift imaging. *Chemistry–A European Journal* **2017**, *23*, 7976-7989.

(14) Binnemans, K. Interpretation of europium(III) spectra. *Coordination Chemistry Reviews* **2015**, *295*, 1-45.

(15) Ungur, L.; Chibotaru, L. F. Ab Initio Crystal Field for Lanthanides. *Chemistry – A European Journal* **2017**, *23*, 3708-3718.

(16) Görller-Walrand, C.; Binnemans, K.: Chapter 155 Rationalization of crystal-field parametrization. In *Handbook on the Physics and Chemistry of Rare Earths*; Elsevier, 1996; Vol. 23; pp 121-283.

(17) Senanayake, P. K.; Rogers, N. J.; Finney, K. L. N.; Harvey, P.; Funk, A. M.; Wilson, J. I.; O'Hogain, D.; Maxwell, R.; Parker, D.; Blamire, A. M. A new paramagnetically shifted imaging probe for MRI. *Magnetic Resonance in Medicine* **2017**, *77*, 1307-1317.

(18) Harnden, A. C.; Parker, D.; Rogers, N. J. Employing paramagnetic shift for responsive MRI probes. *Coordination Chemistry Reviews* **2019**, *383*, 30-42.

(19) Liu, J.; Reta, D.; Cleghorn, J. A.; Yeoh, Y. X.; Ortu, F.; Goodwin, C. A.; Chilton, N. F.; Mills, D. P. Light Lanthanide Metallocenium Cations Exhibiting Weak Equatorial Anion Interactions. *Chemistry–A European Journal* **2019**, *25*, 7749-7758.

(20) Ma, C.-G.; Brik, M.; Kiisk, V.; Kangur, T.; Sildos, I. Spectroscopic and crystal-field analysis of energy levels of Eu3+ in SnO2 in comparison with ZrO2 and TiO2. *Journal of Alloys and Compounds* **2011**, *509*, 3441-3451.

(21) Auzel, F.; Malta, O. A scalar crystal field strength parameter for rare-earth ions: meaning and usefulness. *Journal de Physique* **1983**, *44*, 201-206.

(22) Malta, O.; Antic-Fidancev, E.; Lemaitre-Blaise, M.; Milicic-Tang, A.; Taibi, M. The crystal field strength parameter and the maximum splitting of the 7F1 manifold of the Eu3+ ion in oxides. *Journal of Alloys and Compounds* **1995**, *228*, 41-44.

(23) Gendron, F.; Moore II, B.; Cador, O.; Pointillart, F.; Autschbach, J.; Le Guennic, B. Ab Initio Study of Circular Dichroism and Circularly Polarized Luminescence of Spin-Allowed and Spin-Forbidden Transitions: From Organic Ketones to Lanthanide Complexes. *Journal of Chemical Theory and Computation* **2019**, *15*, 4140-4155.

(24) Souza, A.; Dos Santos, M. C. The J-mixing effect in Ln3+ ions crystal field levels. *Chemical Physics Letters* **2012**, *521*, 138-141.

(25) Jensen, J.; Mackintosh, A. R.: *Rare earth magnetism*; Clarendon Press Oxford, 1991.

(26) Kurzen, H.; Bovigny, L.; Bulloni, C.; Daul, C. Electronic structure and magnetic properties of lanthanide 3+ cations. *Chemical Physics Letters* **2013**, *574*, 129-132.

(27) Hölsä, J.; Lastusaari, M.; Niittykoski, J.; Puche, R. S. Interplay between crystal structure and magnetic susceptibility of tetragonal ROBr. *Physical Chemistry Chemical Physics* **2002**, *4*, 3091-3097.

(28) Butler, S. J.; Delbianco, M.; Lamarque, L.; McMahon, B. K.; Neil, E. R.; Pal, R.; Parker, D.; Walton, J. W.; Zwier, J. M. EuroTracker® dyes: design, synthesis, structure and photophysical properties of very bright europium complexes and their use in bioassays and cellular optical imaging. *Dalton Transactions* **2015**, *44*, 4791-4803.

(29) Delbianco, M.; Sadovnikova, V.; Bourrier, E.; Mathis, G.; Lamarque, L.; Zwier, J. M.; Parker, D. Bright, Highly Water‐Soluble Triazacyclononane Europium Complexes To Detect Ligand Binding with Time‐Resolved FRET Microscopy. *Angewandte Chemie International Edition* **2014**, *53*, 10718-10722.

(30) Shuvaev, S.; Starck, M.; Parker, D. Responsive, Water‐Soluble Europium (III) Luminescent Probes. *Chemistry‐A European Journal* **2017**, *23*, 9974-9989.

(31) Blackburn, O. A.; Edkins, R. M.; Faulkner, S.; Kenwright, A. M.; Parker, D.; Rogers, N. J.; Shuvaev, S. Electromagnetic susceptibility anisotropy and its importance for paramagnetic NMR and optical spectroscopy in lanthanide coordination chemistry. *Dalton Transactions* **2016**, *45*, 6782-6800.

(32) Ofelt, G. Intensities of crystal spectra of rare‐earth ions. *The Journal of Chemical Physics* **1962**, *37*, 511-520.

(33) Judd, B. R. Optical absorption intensities of rare-earth ions. *Physical Review* **1962**, *127*, 750.

(34) Jørgensen, C. K.; Judd, B. Hypersensitive pseudoquadrupole transitions in lanthanides. *Molecular Physics* **1964**, *8*, 281-290.

(35) Piguet, C.; Geraldes, C. F. Paramagnetic NMR lanthanide induced shifts for extracting solution structures. *Handbook on the Physics and Chemistry of Rare Earths* **2003**, *33*, 353-463.

(36) Bertini, I.; Luchinat, C.; Parigi, G. Magnetic susceptibility in paramagnetic NMR. *Progress in Nuclear Magnetic Resonance Spectroscopy* **2002**, *40*, 249.

(37) Funk, A. M.; Finney, K.-L. N.; Harvey, P.; Kenwright, A. M.; Neil, E. R.; Rogers, N. J.; Senanayake, P. K.; Parker, D. Critical analysis of the limitations of Bleaney's theory of magnetic anisotropy in paramagnetic lanthanide coordination complexes. *Chemical Science* **2015**, *6*, 1655-1662.

(38) Castro, G.; Regueiro-Figueroa, M.; Esteban-Gómez, D.; Pérez-Lourido, P.; Platas-Iglesias, C.; Valencia, L. Magnetic anisotropies in rhombic lanthanide (III) complexes do not conform to Bleaney's theory. *Inorganic Chemistry* **2016**, *55*, 3490-3497.

(39) Suturina, E. A.; Mason, K.; Botta, M.; Carniato, F.; Kuprov, I.; Chilton, N. F.; McInnes, E. J.; Vonci, M.; Parker, D. Periodic trends and hidden dynamics of magnetic properties in three series of triazacyclononane lanthanide complexes. *Dalton Transactions* **2019**, *48*, 8400-8409.

(40) Beeby, A.; M. Clarkson, I.; S. Dickins, R.; Faulkner, S.; Parker, D.; Royle, L.; S. de Sousa, A.; A. Gareth Williams, J.; Woods, M. Non-radiative deactivation of the excited states of europium, terbium and ytterbium complexes by proximate energy-matched OH, NH and CH oscillators: an improved luminescence method for establishing solution hydration states. *Journal of the Chemical Society, Perkin Transactions 2* **1999**, 493-504.

(41) Aime, S.; Botta, M.; Parker, D.; Williams, J. G. Extent of hydration of octadentate lanthanide complexes incorporating phosphinate donors: Solution relaxometry and luminescence studies. *Journal of the Chemical Society, Dalton Transactions* **1996**, 17-23.

(42) Woods, M.; Aime, S.; Botta, M.; Howard, J. A.; Moloney, J. M.; Navet, M.; Parker, D.; Port, M.; Rousseaux, O. Correlation of water exchange rate with isomeric composition in diastereoisomeric gadolinium complexes of tetra

(carboxyethyl) dota and related macrocyclic ligands. *Journal of the American Chemical Society* **2000**, *122*, 9781-9792.

(43) Kotek, J.; Rudovský, J.; Hermann, P.; Lukeš, I. Three in One: TSA, TSA ‘, and SA Units in One Crystal Structure of a Yttrium (III) Complex with a Monophosphinated H4dota Analogue. *Inorganic Chemistry* **2006**, *45*, 3097-3102.

(44) Dickins, R. S.; Parker, D.; Bruce, J. I.; Tozer, D. J. Correlation of optical and NMR spectral information with coordination variation for axially symmetric macrocyclic Eu (III) and Yb (III) complexes: axial donor polarisability determines ligand field and cation donor preference. *Dalton Transactions* **2003**, 1264-1271.

(45) Bari, L. D.; Pintacuda, G.; Salvadori, P.; Dickins, R. S.; Parker, D. Effect of axial ligation on the magnetic and electronic properties of lanthanide complexes of octadentate ligands. *Journal of the American Chemical Society* **2000**, *122*, 9257-9264.

(46) Mason, K.; Harnden, A. C.; Patrick, C. W.; Poh, A. W.; Batsanov, A. S.; Suturina, E. A.; Vonci, M.; McInnes, E. J.; Chilton, N. F.; Parker, D. Exquisite sensitivity of the ligand field to solvation and donor polarisability in coordinatively saturated lanthanide complexes. *Chemical Communications* **2018**, *54*, 8486-8489.

(47) Richardson, F. S. On the calculation of electric dipole strengths of 4f→ 4f transitions in lanthanide complexes. *Chemical Physics Letters* **1982**, *86*, 47-50.

(48) Kuroda, R.; Mason, S. F.; Rosini, C. Crystal structure and single-crystal spectra of Gd (Eu) Al 3 (BO 3) 4. Anisotropic ligand polarization contributions to the ƒ–ƒ transition probabilities in Eu III. *Journal of the Chemical Society, Faraday Transactions 2: Molecular and Chemical Physics* **1981**, *77*, 2125-2140.

(49) Lowe, M. P.; Parker, D.; Reany, O.; Aime, S.; Botta, M.; Castellano, G.; Gianolio, E.; Pagliarin, R. pH-dependent modulation of relaxivity and luminescence in macrocyclic gadolinium and europium complexes based on reversible intramolecular sulfonamide ligation. *Journal of the American Chemical Society* **2001**, *123*, 7601-7609.

(50) Krchová, T.; Herynek, V.; Gálisová, A.; Blahut, J.; Hermann, P.; Kotek, J. Eu (III) Complex with DO3A-amino-phosphonate Ligand as a Concentration-Independent pH-Responsive Contrast Agent for Magnetic Resonance Spectroscopy (MRS). *Inorganic Chemistry* **2017**, *56*, 2078-2091.

(51) Shuvaev, S.; Suturina, E. A.; Mason, K.; Parker, D. Chiral probes for α-1-AGP reporting by species-specific induced circularly polarised luminescence. *Chemical Science* **2018**, *9*, 2996-3003.

(52) Rinehart, J. D.; Long, J. R. Exploiting single-ion anisotropy in the design of f-element single-molecule magnets. *Chemical Science* **2011**, *2*, 2078-2085.

(53) Sievers, J. Asphericity of 4f-shells in their Hund's rule ground states. *Zeitschrift für Physik B Condensed Matter* **1982**, *45*, 289-296.

(54) Chilton, N. F.; Collison, D.; McInnes, E. J.; Winpenny, R. E.; Soncini, A. An electrostatic model for the determination of magnetic anisotropy in dysprosium complexes. *Nature Communications* **2013**, *4*, 1-7.

(55) Sorace, L.; Benelli, C.; Gatteschi, D. Lanthanides in molecular magnetism: old tools in a new field. *Chemical Society Reviews* **2011**, *40*, 3092-3104.

(56) Mironov, V. S.; Galyametdinov, Y. G.; Ceulemans, A.; Görller-Walrand, C.; Binnemans, K. Room-temperature magnetic anisotropy of lanthanide complexes: A model study for various coordination polyhedra. *The Journal of Chemical Physics* **2002**, *116*, 4673-4685.

(57) Dai, L.; Zhang, J.; Chen, Y.; Mackenzie, L. E.; Pal, R.; Law, G.-L. Synthesis of Water-Soluble Chiral DOTA Lanthanide Complexes with Predominantly Twisted Square Antiprism Isomers and Circularly Polarized Luminescence. *Inorganic Chemistry* **2019**, *58*, 12506-12510.

(58) Woods, M.; Payne, K. M.; Valente, E. J.; Kucera, B. E.; Young Jr, V. G. Crystal structures of DOTMA chelates from Ce3+ to Yb3+: evidence for a continuum of metal ion hydration states. *Chemistry–A European Journal* **2019**, *25*, 9997-10005.

(59) Mason, S. F.; Peacock, R. D.; Stewart, B. Ligand-polarization contributions to the intensity of hypersensitive trivalent lanthanide transitions. *Molecular Physics* **1975**, *30*, 1829-1841.

(60) Mason, S. F.: The ligand polarization model for the spectra of metal complexes: The dynamic coupling transition probabilities. In *Electrons and Transitions*; Springer, 1980; pp 43-81.

(61) Reid, M. F.; Richardson, F. S. Anisotropic ligand polarizability contributions to lanthanide 4f→ 4f intensity parameters. *Chemical Physics Letters* **1983**, *95*, 501-506.

(62) Poh, A. W.; Aguilar, J. A.; Kenwright, A. M.; Mason, K.; Parker, D. Aggregation of Rare Earth Coordination Complexes in Solution Studied by Paramagnetic and DOSY NMR. *Chemistry–A European Journal* **2018**, *24*, 16170-16175.

(63) McConnell, H. M. Theory of nuclear magnetic shielding in molecules. I. Long‐range dipolar shielding of protons. *The Journal of Chemical Physics* **1957**, *27*, 226-229.

(64) Peters, J.; Huskens, J.; Raber, D. Lanthanide induced shifts and relaxation rate enhancements. *Progress in Nuclear Magnetic Resonance Spectroscopy* **1996**, *28*, 283-350.

(65) Mironov, V. S.; Galyametdinov, Y. G.; Ceulemans, A.; Görller-Walrand, C.; Binnemans, K. Influence of crystal-field perturbations on the room-temperature magnetic anisotropy of lanthanide complexes. *Chemical Physics Letters* **2001**, *345*, 132-140.

(66) McGarvey, B. R. Temperature dependence of the pseudocontact shift in lanthanide shift reagents. *Journal of Magnetic Resonance (1969)* **1979**, *33*, 445-455.

(67) Boulon, M. E.; Cucinotta, G.; Luzon, J.; Degl'Innocenti, C.; Perfetti, M.; Bernot, K.; Calvez, G.; Caneschi, A.; Sessoli, R. Magnetic anisotropy and spin‐parity effect along the series of lanthanide complexes with DOTA. *Angewandte Chemie International Edition* **2013**, *52*, 350-354.

(68) Cucinotta, G.; Perfetti, M.; Luzon, J.; Etienne, M.; Car, P. E.; Caneschi, A.; Calvez, G.; Bernot, K.; Sessoli, R. Magnetic anisotropy in a dysprosium/DOTA single‐molecule magnet: beyond simple magneto‐structural correlations. *Angewandte Chemie International Edition* **2012**, *51*, 1606-1610.

(69) Briganti, M.; Garcia, G. F.; Jung, J.; Sessoli, R.; Le Guennic, B.; Totti, F. Covalency and magnetic anisotropy in lanthanide single molecule magnets: the DyDOTA archetype. *Chemical Science* **2019**, *10*, 7233-7245.

(70) Jung, J.; Islam, M. A.; Pecoraro, V. L.; Mallah, T.; Berthon, C.; Bolvin, H. Derivation of lanthanide series crystal field parameters from first principles. *Chemistry–A European Journal* **2019**, *25*, 15112-15122.

(71) Ungur, L.; Chibotaru, L. F. Ab initio crystal field for lanthanides. *Chemistry–A European Journal* **2017**, *23*, 3708-3718.

(72) Golding, R.; Pyykkö, P. On the theory of pseudocontact NMR shifts due to lanthanide complexes. *Molecular Physics* **1973**, *26*, 1389-1396.

(73) Charnock, G.; Kuprov, I. A partial differential equation for pseudocontact shift. *Physical Chemistry Chemical Physics* **2014**, *16*, 20184-20189.

(74) Suturina, E. A.; Kuprov, I. Pseudocontact shifts from mobile spin labels. *Physical Chemistry Chemical Physics* **2016**, *18*, 26412-26422.

(75) Golding, R.; Halton, M. A theoretical study of the ¹⁴N and ¹⁷O N.M.R. shifts in lanthanide complexes. *Australian Journal of Chemistry* **1972**, *25*, 2577-2581.

(76) Reilley, C. N.; Good, B. W.; Allendoerfer, R. D. Separation of contact and dipolar lanthanide induced nuclear magnetic resonance shifts: evaluation and application of some structure independent methods. *Analytical Chemistry* **1976**, *48*, 1446-1458.

(77) Kreidt, E.; Bischof, C.; Platas-Iglesias, C.; Seitz, M. Magnetic Anisotropy in Functionalized Bipyridyl Cryptates. *Inorganic Chemistry* **2016**, *55*, 5549-5557.

(78) Esteban-Gómez, D.; Büldt, L. A.; Pérez-Lourido, P.; Valencia, L.; Seitz, M.; Platas-Iglesias, C. Understanding the Optical and Magnetic Properties of Ytterbium (III) Complexes. *Inorganic Chemistry* **2019**, *58*, 3732-3743.

(79) Parigi, G.; Benda, L.; Ravera, E.; Romanelli, M.; Luchinat, C. Pseudocontact shifts and paramagnetic susceptibility in semiempirical and quantum chemistry theories. *The Journal of Chemical Physics* **2019**, *150*, 144101.

(80) Benda, L.; Mareš, J.; Ravera, E.; Parigi, G.; Luchinat, C.; Kaupp, M.; Vaara, J. Pseudo‐Contact NMR Shifts over the Paramagnetic Metalloprotein CoMMP‐12 from First Principles. *Angewandte Chemie International Edition* **2016**, *55*, 14713-14717.

(81) Benda, L.; Mareš, J.; Ravera, E.; Parigi, G.; Luchinat, C.; Kaupp, M.; Vaara, J. Pseudo-Contact NMR Shifts over the Paramagnetic Metalloprotein CoMMP-12 from First Principles. *Angewandte Chemie* **2016**, *128*, 14933-14937.

(82) Hogben, H.; Krzystyniak, M.; Charnock, G.; Hore, P.; Kuprov, I. Spinach–a software library for simulation of spin dynamics in large spin systems. *Journal of Magnetic Resonance* **2011**, *208*, 179-194.

(83) Mason, K.; Rogers, N. J.; Suturina, E. A.; Kuprov, I.; Aguilar, J. A.; Batsanov, A. S.; Yufit, D. S.; Parker, D. PARASHIFT probes: solution NMR and X-ray structural studies of macrocyclic ytterbium and yttrium complexes. *Inorganic Chemistry* **2017**, *56*, 4028-4038.

(84) Vonci, M.; Mason, K.; Neil, E. R.; Yufit, D. S.; McInnes, E. J.; Parker, D.; Chilton, N. F. Sensitivity of Magnetic Anisotropy in the Solid State for Lanthanide Complexes with Small Crystal Field Splitting. *Inorganic Chemistry* **2019**, *58*, 5733-5745.

(85) Bertini, I.; Luchinat, C.; Parigi, G.; Pierattelli, R. NMR spectroscopy of paramagnetic metalloproteins. *ChemBioChem* **2005**, *6*, 1536-1549.

(86) Otting, G. Protein NMR using paramagnetic ions. *Annual review of biophysics* **2010**, *39*, 387-405.

(87) Suturina, E. A.; Häussinger, D.; Zimmermann, K.; Garbuio, L.; Yulikov, M.; Jeschke, G.; Kuprov, I. Model-free extraction of spin label position distributions from pseudocontact shift data. *Chemical science* **2017**, *8*, 2751-2757.

(88) Caravan, P. Protein-targeted gadolinium-based magnetic resonance imaging (MRI) contrast agents: design and mechanism of action. *Accounts of Chemical Research* **2009**, *42*, 851-862.

(89) Clore, G. M.; Iwahara, J. Theory, practice, and applications of paramagnetic relaxation enhancement for the characterization of transient low-population states of biological macromolecules and their complexes. *Chemical Reviews* **2009**, *109*, 4108-4139.

(90) Vega, A. J.; Fiat, D. Nuclear relaxation processes of paramagnetic complexes the slow-motion case. *Molecular Physics* **1976**, *31*, 347-355.

(91) Guéron, M. Nuclear relaxation in macromolecules by paramagnetic ions: a novel mechanism. *Journal of Magnetic Resonance (1969)* **1975**, *19*, 58-66.

(92) Bloembergen, N. Proton relaxation times in paramagnetic solutions. *The Journal of Chemical Physics* **1957**, *27*, 572-573.

(93) Funk, A. M.; Harvey, P.; Finney, K.-L. N.; Fox, M. A.; Kenwright, A. M.; Rogers, N. J.; Senanayake, P. K.; Parker, D. Challenging lanthanide relaxation theory: erbium and thulium complexes that show NMR relaxation rates faster than dysprosium and terbium analogues. *Physical Chemistry Chemical Physics* **2015**, *17*, 16507-16511.

(94) Rogers, N. J.; Finney, K.-L. N.; Senanayake, P. K.; Parker, D. Another challenge to paramagnetic relaxation theory: a study of paramagnetic proton NMR relaxation in closely related series of pyridine-derivatised dysprosium complexes. *Physical Chemistry Chemical Physics* **2016**, *18*, 4370-4375.

(95) Funk, A. M.; Fries, P. H.; Harvey, P.; Kenwright, A. M.; Parker, D. Experimental measurement and theoretical assessment of fast lanthanide electronic relaxation in solution with four series of isostructural complexes. *The Journal of Physical Chemistry A* **2013**, *117*, 905-917.